6th AIAA Flow Control Conference
25 - 28 June 2012, New Orleans, Louisiana

AIAA 2012-2810

Control of Oblique Shock Wave-Boundary Layer Interactions Using Plasma Actuators

N. Webb[1], C. Clifford[2], and M. Samimy[3]

Gas Dynamics and Turbulence Laboratory
Aeronautical and Astronautical Research Laboratories
The Ohio State University
2300 West Case Road
Columbus, OH 43235

Mixed-compression inlets incorporate oblique shock trains in order to efficiently compress incoming flow, resulting in multiple shock wave/boundary layer interactions (SWBLIs). Due to detrimental consequences of SWBLIs (increased distortion and unsteadiness, unstart), boundary layer bleed has traditionally been used to mitigate the interaction. The increased inlet size, and consequently increased weight and drag, necessary to compensate for the bleed mass flow makes bleed undesirable. In the present work localized arc filament plasma actuators (LAFPAs) are used for SWBLI control. The LAFPAs are used in an oblique impinging SWBLI and their control authority is investigated. The LAFPAs are observed to have significant control authority to displace the reflected shock and most of the interaction upstream by approximately one boundary layer thickness. An investigation of the effect of actuator placement, frequency, and duty cycle on the control authority seems to indicate that the actuators' primary control mechanism is Joule heating.

Nomenclature

U_∞ = upstream freestream velocity (m/s)
δ = upstream boundary layer thickness (mm)
δ^* = upstream boundary layer displacement thickness, subscript "*i*" indicates incompressible (mm)
θ = upstream boundary layer momentum thickness, subscript "*i*" indicates incompressible (mm)
H = upstream boundary layer shape factor, subscript "*i*" indicates incompressible (δ^*/θ)
L_{int} = interaction length (mm)
St = Strouhal number, normalized frequency: $f L_{int} / U_\infty$
St_F = Strouhal number at which the actuators were operated
X_o = streamwise location of the projected primary shock inviscid impingement point
X^* = normalized streamwise coordinate: $(X - X_o)/L_{int}$
$X_a{}^*$ = normalized streamwise location of the actuators

Introduction

Supersonic air breathing propulsion is a difficult endeavor with many technical challenges. One of these lies in efficiently ingesting air to be used in the combustion and propulsion processes. The primary aim of this process has long been to collect the air "with the least possible loss in total pressure or head, with the best attainable flow distribution, and with the least amount of aircraft drag." [1] This can be accomplished most efficiently by mixed-compression inlets, which make use of both internal and external compression. This configuration allows the inlet to maximize the number of oblique shocks used to compress the flow, thereby minimizing the total pressure loss. An additional advantage of mixed compression inlets is their superior acoustic properties compared to external compression inlets. Mixed compression inlets also have some drawbacks; in particular, the internal shock reflections

[1] Graduate Student, Department of Mechanical and Aerospace Engineering
[2] Graduate Student, Department of Mechanical and Aerospace Engineering
[3] John B. Nordholt Professor of Mechanical and Aerospace Engineering, AIAA Fellow, Email: Samimy.1@osu.edu

result in multiple interactions between shocks and the internal inlet surface boundary layer. Such interactions are commonly referred to as shock wave-boundary layer interactions (SWBLIs).

These interactions impose sharp adverse pressure gradients on the developing boundary layer severely degrading it and, if the interaction strength is sufficient, causing separation. Figure 1 is a schematic of a separated SWBLI. In either case inlet total pressure recovery is reduced and flow distortion increased. Under severe circumstances boundary layer separation can introduce sufficient aerodynamic blockage to cause unstart. The constant performance detriment combined with the potential for severe consequences make SWBLI control an important part of mixed-compression inlet design. Traditionally boundary layer bleed has been used to exert this control.[2] Scoops, slots, and holes are used to remove low momentum boundary layer fluid avoiding severe SWBLIs altogether. Bleed serves as more than just a separation control mechanism; it also reduces distortion at the aerodynamic interface plane by removing the boundary layer and allows the inlet/engine more flexibility by providing a mechanism for balancing inlet capture mass flow with the engine demand.[3]

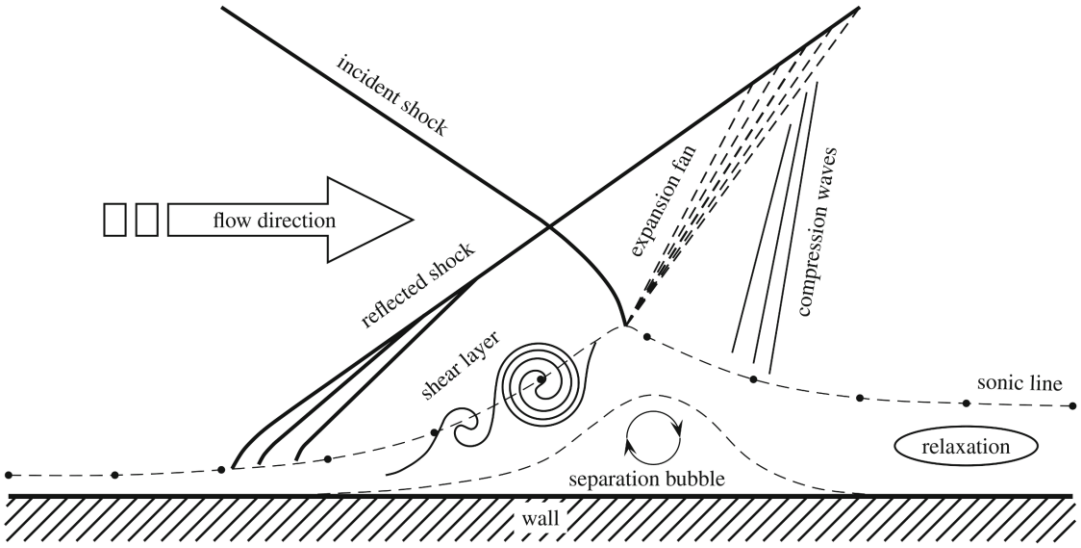

Figure 1: Schematic of a SWBLI with Separation[4]

Despite all the benefits of boundary layer bleed, there are associated performance detriments. Removal of captured mass flow necessitates a larger initial mass capture by the inlet to supply engine requirements. This mandates increased capture area, which yields a heavier inlet with greater drag. Furthermore, the bled mass flow must be dumped overboard adding to the bleed-drag penalty. The weight/drag penalty makes minimization of bleed desirable from an overall inlet efficiency standpoint. Although separation control devices cannot fully replace bleed, due to its multiple benefits[3], they can still improve the overall performance of the inlet by minimizing the amount of bled mass flow.

To this end, the research community has been investigating a variety of separation control techniques for SWBLIs (both on transonic wings and in mixed-compression inlets). Both passive and active techniques are being explored, one of the most prominent being vortex generators. These have been explored in a variety of shapes and sizes from large scale (height ~ δ)[5] to so-called micro-vortex generators: micro-vanes[6], ramps[7,8], hybrid geometries[9], and other configurations. These studies seek to improve boundary layer response to the shock-imposed pressure gradient by using streamwise vorticity to enhance mixing, thus increasing velocity in the near-wall region. Vortex generator research also focuses on minimizing the inherent drag associated with these devices. Three-dimensional bumps have also been explored for SWBLI control. Babinsky and Ogawa[10] have investigated their ability to smear/spread the shock impingement of a normal SWBLI to ease the sharp pressure gradient imposed on the boundary layer. An additional benefit of the bumps is that spreading the shock structure decreases total pressure loss through the shock system. Another passive flow control technique is the use of meso-flaps designed to impart momentum to the boundary layer.[11]

Passive control is attractive because it does not require energy input or (usually) moving parts. Thus, these flow control techniques are commonly robust and require minimal maintenance. The drawback is that the control is usually only effective near design conditions. Moreover, the presence of geometric modifications at off-design conditions still generates parasitic drag (and perhaps worse effects) even when no benefits are present. Although

boundary layer bleed is relatively flexible, this quality is far from typical among passive control techniques. Active flow control can sometimes address this issue. Although it requires energy to function, and consequently imposes a parasitic drain on system resources; its nature often allows it to be much more flexible than passive control: turning off when under off-design conditions, or even adjusting to regain control authority at the new condition. Researchers have also examined active control methods for separation control in SWBLIs. Kalra et al.[12] investigated the use of magnetohydrodynamic actuators (a.k.a. "snow-plow arcs") to add momentum to the near wall flow, thereby delaying separation. Micro-jets[13] and zero-net-mass-flux spark jets[14] have also been used to act as virtual/ aerodynamic vortex generators. These generators could be turned on/off or altered based on flow conditions. Continuous or pulsed blowing has also been considered as a method of adding momentum to the boundary layer.

In addition to directly controlling the flow, active control can be used to introduce perturbations to the flow. These perturbations can be organized to exploit naturally occurring instabilities in the flow. This can either change the flow structure through instability modification, or amplify the perturbations to significant structures using natural instabilities. Natural instabilities often manifest themselves in flow unsteadiness. Thus natural unsteadiness in SWBLIs could indicate the presence of natural instabilities. Turbulence does result in minor unsteadiness in SWBLIs; however the unsteadiness amplitude increases dramatically in separated interactions. A low-frequency unsteadiness has been observed in the region around the reflected shock.[4,15,16] This unsteadiness is broadband in nature, but centers about a frequency approximately two orders of magnitude lower than the freestream turbulence.

Researchers have long sought the source of this unsteadiness.[17] Historically there have been two primary theories: 1) That upstream perturbations cause the low frequency motion, and 2) That downstream perturbations are responsible. There have been a variety of researchers who have examined the upstream boundary layer seeking to correlate the shock movement to various events such as bursting[18] or streamwise elongated structures.[19,20] Those who lean more towards the downstream influence theories focus on the separation region. Pipponiau et al.[21] proposed that periodic vortex shedding from the shear layer over the separation bubble causes a low frequency expansion/contraction of the separation bubble, pushing the shock upstream and subsequently allowing it to relax downstream. This could attribute the reflected shock unsteadiness to a Kelvin-Helmholtz type instability. Other theories propose an acoustic feedback loop in the separated region[22], or a global instability.[4] Recent work by Narayanswamy[23] seems to indicate that neither upstream nor downstream influences are solely responsible for the unsteadiness, rather a combination of the two. Upstream influence appears to be significant for incipiently or weakly separated interactions, while the downstream influences become dominant for stronger interactions. Analytical work by Touber and Sandham[24] also seems to indicate that, instead of being due to any particular perturbation, the unsteadiness is inherent to the coupled shock-boundary layer equations and is the natural manifestation of the perturbed system.

The various theories of potential instabilities suggest many potential manners in which excitation of flow instabilities could improve (or deteriorate) the flow. For example separation vortex shedding might be accelerated or the structure size amplified by properly seeding the shear layer with perturbations, potentially reducing/eliminating separation.[25,26] Another possibility is that the natural instability could be regularized or accentuated to decrease the broadband nature of the oscillation. Due to the detrimental effect on aircraft components that can be caused by SWBLI unsteadiness[27] this could ease, or more clearly define, the fatigue requirements for those components.

Localized Arc Filament Plasma Actuators (LAFPAs) were developed at The Ohio State University specifically for strong, high frequency perturbation introduction.[28] This allows them to perturb a wide variety of flows. A significant amount of work has been done on LAFPAs as a noise mitigation and mixing enhancement control technique for high-speed, high-Reynolds number jets.[29,30] The flexibility and dynamic nature of the LAFPAs also allows them to be used in a feedback control loop for real-time feedback control.[31] Considering the presence of natural instabilities in SWBLIs, it was decided to investigate the LAFPAs' effectiveness for separation control in a SWBLI. Although as discussed in Titchener et al.[32], a single SWBLI may not be a realistic model of a mixed compression inlet, which contains multiple SWBLIs and other types of adverse pressure gradients, a unit problem (single oblique impinging SWBLI) seemed a good starting point to verify the potential of LAFPAs for SWBLI separation control.

Previously the LAFPAs' fitness for separation control in a SWBLI had been investigated.[33] After detecting potential in the LAFPAs a more in-depth work was begun by expanding the facility and its measurement capabilities.[34] The present work continues to explore the LAFPAs' potential control authority in a SWBLI. The paper details modifications to the new test facility, and a characterization of the baseline. Centerline velocity measurements of the flow using PIV for various forcing cases are presented and analyzed, and a potential control mechanism is discussed.

Experimental Methodology

A. Physical Arrangement

As previously discussed it was deemed appropriate to explore the separation control authority of the LAFPAs in a single oblique impinging SWBLI. The preliminary test facility was expanded[34] to that used for this work. It is a blow-down facility that uses compressed, dried air from large (~36 m^3) storage tanks. The stagnation to ambient pressure difference is controlled through a variable valve and electronic feedback control system. The test section is rectangular, 3 in. by 2.87 in., the freestream Mach number is 2.33, and the stagnation temperature is approximately ambient. Optical access to the test section was provided by two nominally 3 in. high by 10 in. long fused quartz windows. A slit window in the test section ceiling allows for a centerline streamwise-vertical laser sheet. The facility described by Webb et al.[34] uses a variable angle wedge to generate the primary impinging shock. The preliminary work used a 10° compression ramp to generate the primary shock. In order to eliminate possible experimental confounds, a Variable Compression Ramp (VCR) was designed for the expanded wind tunnel. The VCR is a 10° compression ramp that can be installed in three streamwise locations. This allows the streamwise location of the LAFPAs to be varied with respect to the SWBLI. Figure 2 is a schematic of the test section of the wind tunnel used in this work.

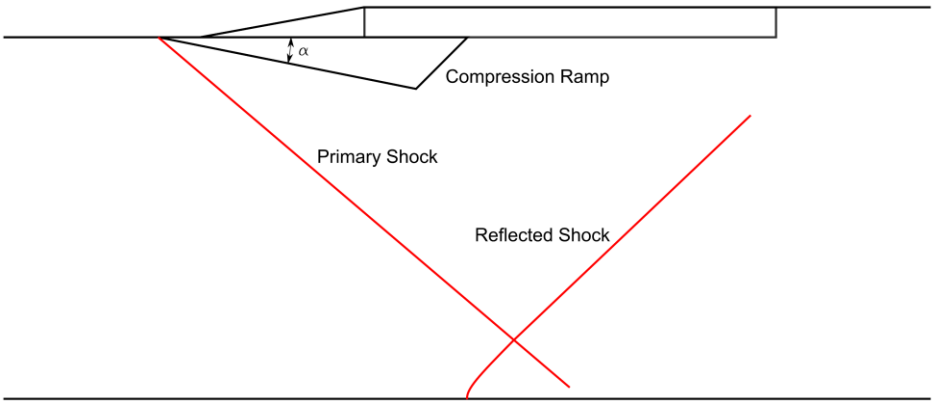

Figure 2: Test Section Schematic with Compression Ramp Model Installed

Each LAFPAs' physical configuration is two tungsten electrodes mounted with the tips flush to the tunnel floor. The electrodes protrude from a 1 mm wide by 0.5 mm deep groove in the tunnel floor. After air breakdown and formation of a plasma arc, this groove shields the arc and allows it to achieve a quasi-steady condition. The tips of the electrodes are separated by 3 mm center-to-center, with a 5 mm separation between the nearest electrodes of two different actuators. Eight actuators are arranged in line across the span of the test section. The electrodes are configured such that the flow is normal to the line of electrodes/actuators. Figure 3 shows a diagram of the LAFPAs' physical arrangement.

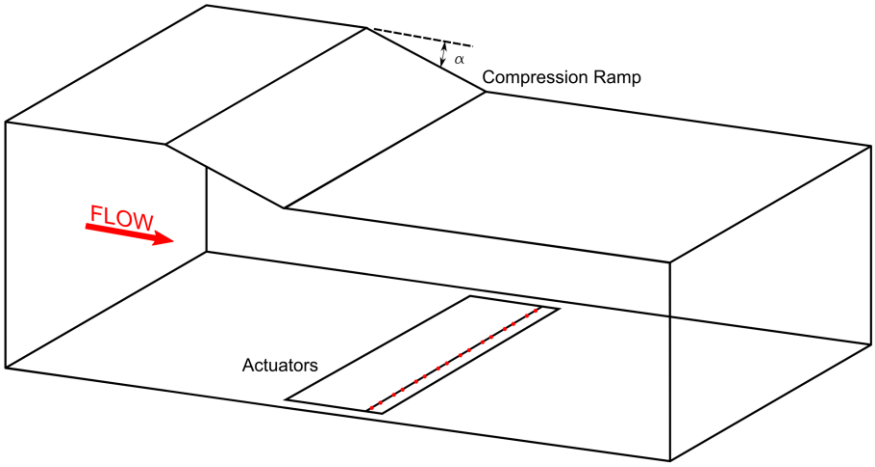

Figure 3: Schematic of LAFPA Arrangement

The actuators are operated by rapidly applying a high voltage across the electrodes. This induces breakdown in the air between the electrodes and a localized arc filament forms. The arc produces rapid localized heating generating a thermal (followed by a pressure) perturbation in the flow that can be used for flow control. The power supply used in this work[28] allows the cycle of breakdown, quasi-steady arc formation, and shutdown to be repeated at a variable frequency up to 200 kHz. The physical configuration of the electrodes results in steady state arc formation with about a 400 V differential and 0.25 A current. Although the peak power release (immediately following breakdown) is much greater than the approximately time average power of 50 W (for 50% duty cycle), for the relatively low frequencies ($\leq$ 20 kHz) used in this study, the peak power release contributes a negligible amount to the time averaged power. The time averaged power input varies based on the duty cycle (percent of a period during which the actuators are firing), e.g. for a 30% duty cycle the power release will be approximately 30 W per actuator. For the majority of this work the duty cycle was 50%, which means that the released power was approximately 400 W for the 8 actuators used in this work. This is 0.13% of the inviscid flow power.

B. Flow Diagnostics

Qualitative flow characterization was performed using schlieren imaging. Schlieren (as a density gradient based measurement technique) primarily provides data regarding the wave structure. This allows the baseline flow to be observed and confirmed as the desired flow. Additionally the interaction length can be measured. Moreover any changes in the wave structure due to the LAFPAs can be observed using this fast, easy, low-cost measurement technique. Schlieren also supplies a qualitative metric of the general quality and cleanliness of the flow.

Surface Oil Flow Visualization (SOFV) added qualitative information regarding the interaction shape across the tunnel span. The oil used was a mixture of gear oil, oil paint pigment, and oleic acid (an anti-coagulant). A thin coat of oil was applied to the test section floor and the flow was started as quickly as possible. The primary purpose of the SOFV was to supplement the largely centerline measurements used in this study with the full three-dimensional signature of the interaction region on the test section surface.

Two component Particle Image Velocimetry (PIV) on a streamwise-vertical plane was the primary data metric for the forced cases. It gives quantitative data regarding the changes in the interaction introduced by the LAFPAs. The PIV data was acquired using the commercially available DaVis 7.2 PIV software and a LaVision Imager Pro X camera. Illumination was provided by a Spectra Physics Quanta-Ray PIV 400 laser. Cross-correlation and post processing was performed by DaVis. MATLAB was used to average, organize, and otherwise reduce the data.

Real-time pressure measurements on the tunnel centerline allowed the SWBLI unsteadiness to be quantitatively examined and compared to literature. The pressure measurements were collected by Kulite XTL-140-25A pressure transducers. The data was acquired at 50 kHz and an analog hardware low-pass filter was applied with a filter frequency of 25 kHz. The data were taken in de-correlated blocks of 4096 samples which yields a lowest resolvable frequency of 12.2 Hz. 200 blocks of data were taken for each measurement. Spectra of the data were generated in MATLAB and all weighting, normalizing, etc. was performed in MATLAB.

C. Experimental Approach

The primary purpose of this work is to expand the investigation of the LAFPAs' ability to provide separation control for supersonic inlets. The hypothesized control mechanism is the potential manipulation of natural instabilities by the introduction of appropriate perturbations. The Kelvin-Helmholtz instability proposed by Piponniau et al.[21] is particularly intriguing because of its direct relationship to the size of the separation region. The separation could potentially be mitigated by manipulating the instability. Using this hypothesis as a starting point, the investigation was begun by forcing the appropriate location and frequency. The sensitive location for shear layer instabilities is usually the shear layer origin. Therefore the LAFPAs were located near the upstream end of the interaction (upstream of the separation line) to allow the perturbations to be convected directly to the hypothesized sensitive region. The most intuitive frequency at which to operate the LAFPAs is that of the natural instability: $St = 0.03$. This corresponds to the parameters which yielded the most control authority in the original investigation.[33]

These forcing parameters were used as an initial investigation step. From there both actuator location and frequency were varied, and the effect on the SWBLI observed. Additionally other forcing parameters, such as duty cycle, were varied to determine their effect on the flow. Based on the response of the flow further testing with a variety of parameters was conducted in an attempt to better understand the LAFPAs' effects on the flow.

Results and Discussion

D. Baseline Characterization

Before examining the LAFPAs' control authority the baseline flow was characterized. It was also of interest to observe the differences in unsteadiness between the variable angle wedge interaction and the VCR interaction. Schlieren imaging provided quick qualitative data of the test section flow. It was used to confirm that flow was started and was reaching the desired/expected condition. Figure 4 shows a mean schlieren image. The schlieren images also contain information regarding any region with moderate density gradient, in particular the wave structure. This allows the interaction length to be determined, defined here as the distance between the (mean) reflected shock foot and the inviscid, primary shock impingement location. This was measured to be 39 mm. The interaction length is used in defining the Strouhal number of the potential unsteady behavior of the interaction region and the forcing frequency. This method of frequency normalization, involving the freestream velocity and the interaction length, has been shown to collapse unsteadiness frequency from a wide variety of interactions to similar values.[16]

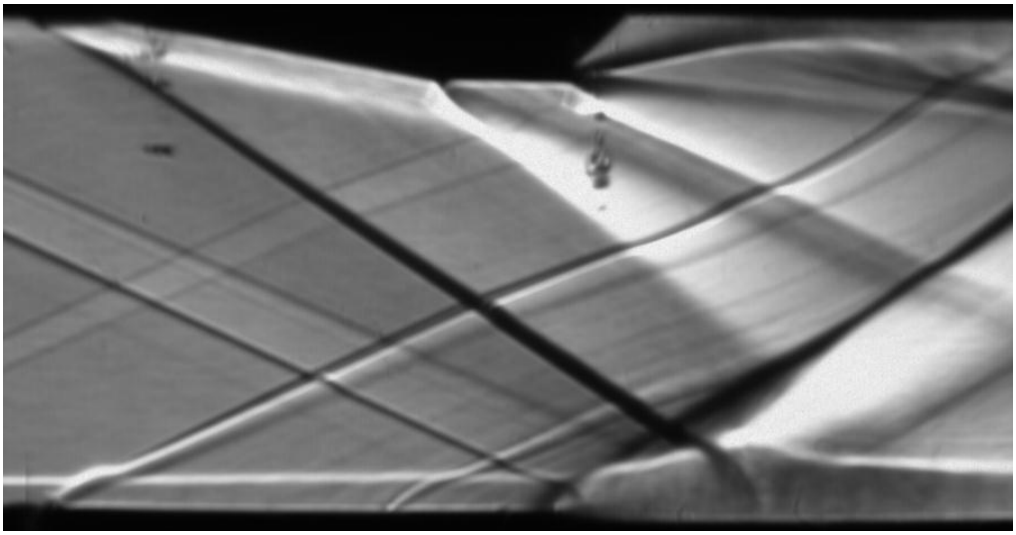

Figure 4: Baseline Mean Schlieren Image

Corner flows have been shown to have significant influence on the size/separation severity of the nominally two-dimensional region of the interaction.[35,36] Most of the flow diagnostics used in this study (schlieren, streamwise PIV, real-time pressure measurements) record conditions only along the tunnel centerline, or integrated across the tunnel span. SOFV provided information regarding the corner flows. It has been observed that large corner interactions tend to mitigate the centerline separation and vice versa.[35] Thus the ratio of the nominally two-dimensional region of the interaction to the test section span can provide a clearer idea of the interaction strength. An annotated SOFV image is shown in Figure 5. The centerline interaction spans 50% to 60% of the tunnel. This likely indicates that the nominally two-dimensional portion of the interaction is milder than it would be in an axisymmetric configuration.

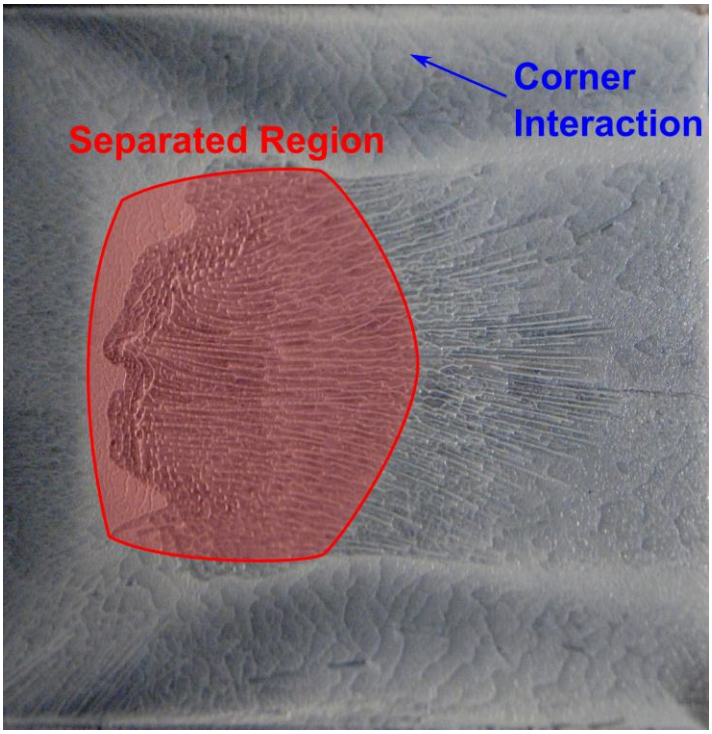

Figure 5: Annotated Mean Surface Oil Flow Visualization Image

SOFV also clearly verified the presence of separation. None of the other flow metrics used were able to detect the separation due to its small vertical dimension. SOFV revealed an interaction shaped similarly to that of the thin to moderate boundary layer case observed by Baruzzini et al.[37] In particular the separation line appeared to be relatively two-dimensional, while reattachment was much more three-dimensional.

Streamwise PIV measurements on the tunnel centerline provided a quantitative view of the interaction. One of the reasons for moving to a larger facility was to push the expansion fan from the downstream end of the shock generator further downstream. [34] Although the larger facility did move it further downstream, it still impinges on the recovering boundary layer relatively close to the trailing end of the interaction. As a result, the downstream profiles may not accurately reflect how the boundary layer would recover because of the imposed favorable pressure gradient. However, the presence of the expansion fan in both the baseline and forced cases allows a direct comparison of the recovering boundary layers. Thus, the actuators' effect on the boundary layer recovery after the interaction can be investigated semi-quantitatively using PIV.

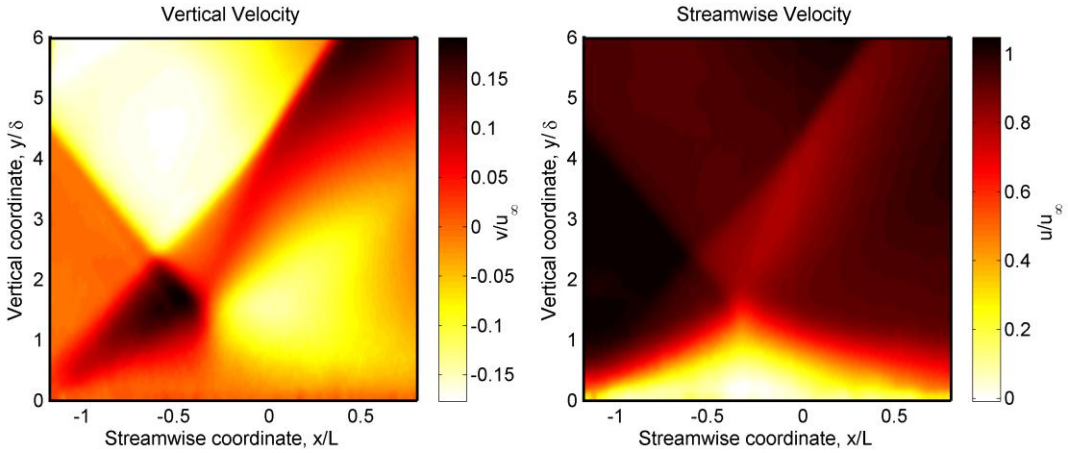

Figure 6: Streamwise and Vertical Mean Velocity Maps on the Test Section Centerline

Upstream boundary layer data can also be obtained from PIV. The state of the incoming boundary layer, in addition to the shock strength and sidewall boundary layer (corner flows), is crucial to determining the interaction size, shape, severity, unsteadiness, etc. Thus, a characterization of it is essential to fully understand the interaction in which the LAFPAs are being tested. Table 1 details freestream flow properties and upstream boundary layer properties. The boundary layer thickness (δ) is defined based on a $0.99U_\infty$ criterion and the integral thicknesses are calculated in the incompressible manner, although the compressible values are included for completeness. When calculating the compressible values the density profile was estimated using the technique proposed in Maise and McDonald.[38] The choice of incompressible statistics yields a more widely used value (pp. 21 [39]). The boundary layer nature (laminar, transitional, or turbulent) is also an important part of determining its condition. Due to the long distance over which the boundary layer developed, it was assumed to be turbulent. Maise and McDonald[38] developed a model profile for turbulent, compressible, adiabatic boundary layers. This profile uses the van Driest transformation to collapse boundary layers with a variety of freestream Mach numbers to a single profile. See Webb et al.[34] for the application of the van Driest transform. A comparison of the van Driest transform of the upstream boundary layer profile to the model profile is shown in Figure 7. The observed excellent agreement is a strong indication that the incoming boundary layer is fully turbulent.

Table 1: Upstream Boundary Layer Properties

M_∞	u_∞ (m/s)	δ (mm)	δ_i^* (mm)	θ_i (mm)	H_i	δ^* (mm)	θ (mm)	H
2.33	559	5.35	1.40	0.78	1.79	2.28	0.53	4.27

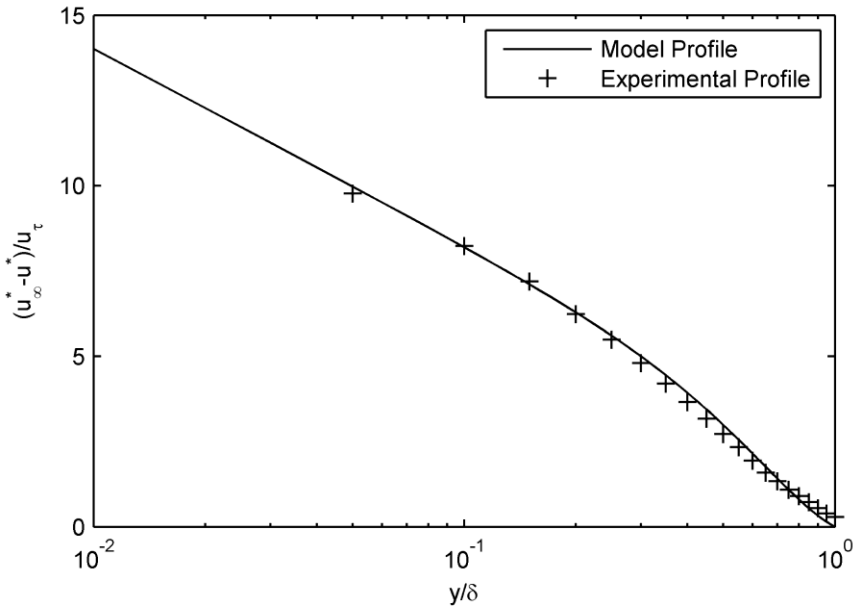

Figure 7: Velocity Profile Using van Driest Transformation and Maise and McDonald[38] Model Profile

As previously mentioned the centerline real-time pressure measurements are of special interest to see whether the unsteady nature of the interaction region depends on the nature of its generation. Previously the unsteadiness of the VAW generated interaction was observed to match the literature quite well.[34] Figure 8 shows the unsteadiness data for the VCR generated interaction. The weighting and normalization of the PSD curves was carried out as described in Dupont et al.[16] It should be noted that the area beneath each curve is unity; therefore the amplitude of the fluctuations cannot be compared from one streamwise location to another. The purpose of this plot is to observe how the most energetic frequency changes at different locations within the interaction. Comparing these results to the previous work[34] shows that the changed shock generator does not appear to have any significant effect on the interaction unsteadiness. The salient features observed in literature, 1) peak energy content around St = 0.03 in the reflected shock impingement region, and 2) peak energy content around St = 0.5 in the downstream regions of the interaction, are present in both cases. The only notable difference between this and the previous work is that here, the transition to higher frequencies appears to take place further downstream within the interaction. However, this location is more consistent with literature.[4,16]

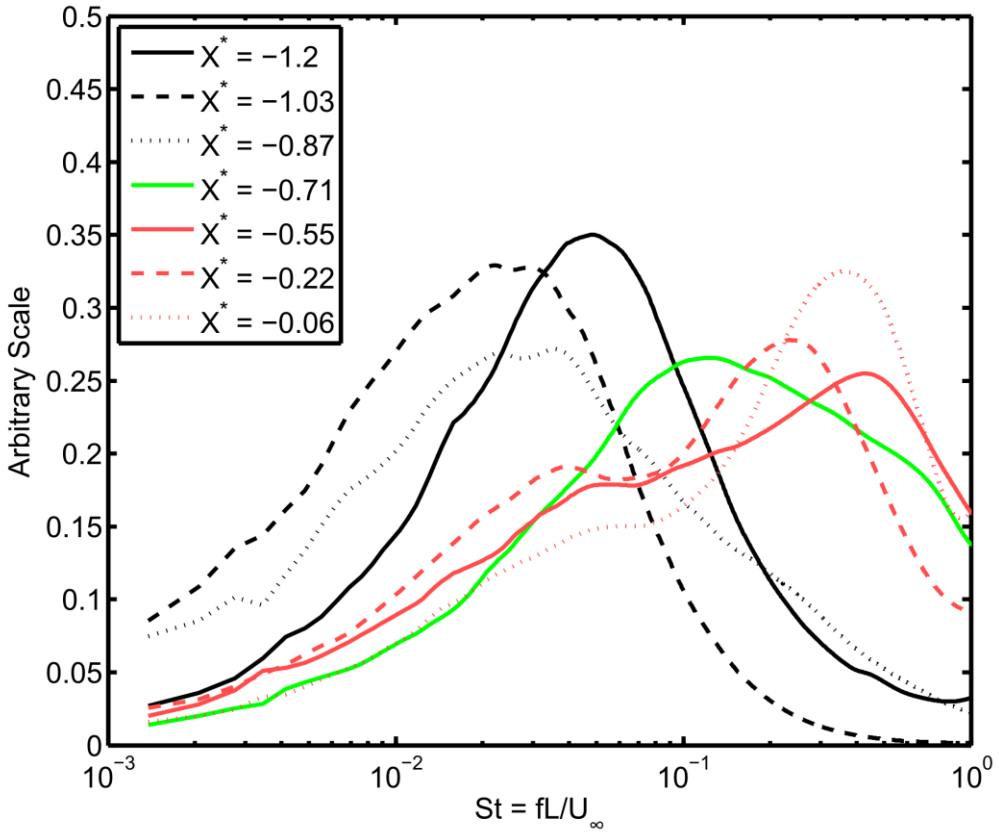

Figure 8: Weighted and Normalized PSD Plots of SWBLI Unsteadiness at Various Streamwise Locations

The real-time pressure measurements were also performed to determine initial actuation parameters. As previously mentioned the starting assumption for this investigation is that the LAFPAs' perturbations would manipulate the shear layer instabilities in order to control the interaction process. The shear layer vortex shedding has been suggested to be the source of the low frequency unsteadiness of the reflected shock.[21] Thus, the pressure data from this region is a direct measure of the peak frequency of this unsteadiness and potential instability. This provided a starting point in the forcing parameter space.

E. LAFPA Control Authority

Having completed the characterization of the baseline flow the LAFPAs' effectiveness was examined. According to the previously determined initial parameters the LAFPAs were placed at a streamwise location of $X_a^* = -0.83$ (see Figure 11), and operated at $St_F = 0.03$ in-phase. PIV data provided the primary quantitative measure of the effects of the LAFPAs. In order to accentuate the differences caused by the actuators the velocity maps of the baseline (Figure 6) were subtracted from those of the forced case. The maps of velocity difference are shown in Figure 9. The immediately obvious effect of the actuators, when these images are compared with those of the baseline, is to move the reflected shock upstream of its baseline location. A careful examination of Figure 9 also shows that the interaction region seems to be moving upstream slightly. Other than a positional shift, the velocity maps for the forced case are nearly identical to those of the baseline. In particular, the interaction region does not seem to be energized or reduced in size; neither has it been enlarged. This differs from the findings of the initial study where the LAFPAs were observed to energize the flow within the interaction region.[33] It is most likely that the shift in the interaction region along with a spanwise viewing plane caused the data in the initial study to be misinterpreted. This conclusion is further reinforced by the observance of a similar shift in the reflected shock for the forced VAW cases.

The reflected shock movement is much more apparent in the vertical velocity difference map. For this reason, only the vertical velocity difference will be displayed from this point on.

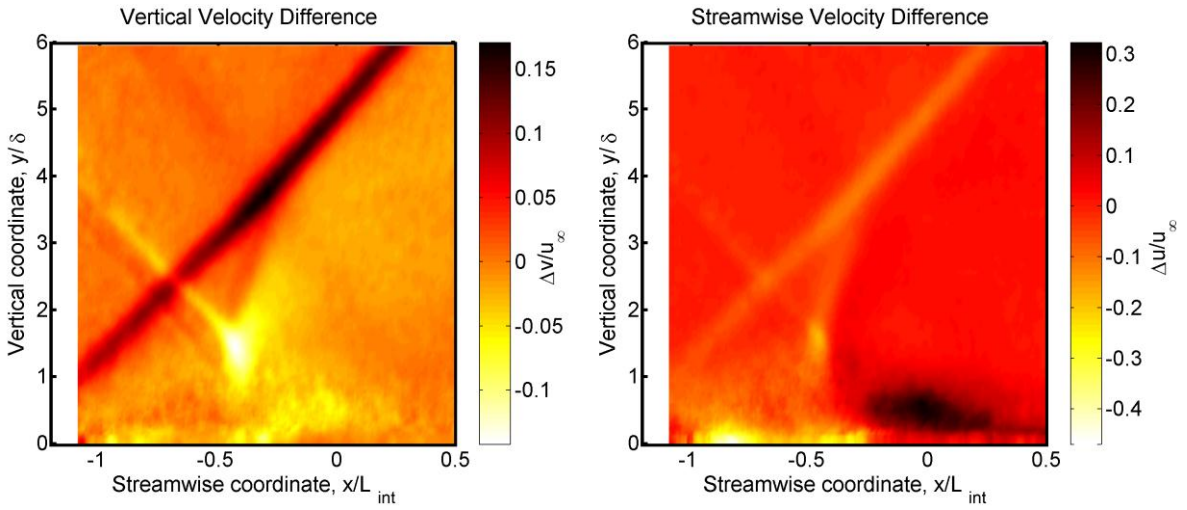

Figure 9: Velocity Difference Images with Forcing Strouhal Number St_F = 0.03.

While the apparent shift of the interaction upstream shows the significant authority of LAFPAs on a SWBLI, it is not an obviously useful modification. Phase-locked PIV was therefore used to gain further insight into what was occurring. This involved locking the PIV acquisition to a particular phase in the LAFPA forcing period, e.g. 0° - just begun firing, 180° - just stopped firing (for 50% duty cycle). This allowed the collection of data that showed what the interaction looked like, on phase-averaged basis, at different points throughout the forcing period. Figure 10 shows the results of an equally distributed eight-phase sweep at the initial forcing conditions. The LAFPAs have just begun firing in phase 1 (Figure 10a) and just stopped firing in phase 5 (Figure 10e). A careful comparison of the various phases reveals that the reflected shock begins to move upstream as soon as the LAFPAs fire, and continues to do so until the actuators stop firing. The shock then begins to relax back toward its baseline location. This frequency, however, does not appear to allow sufficient time for the shock to relax completely before the next forcing period begins.

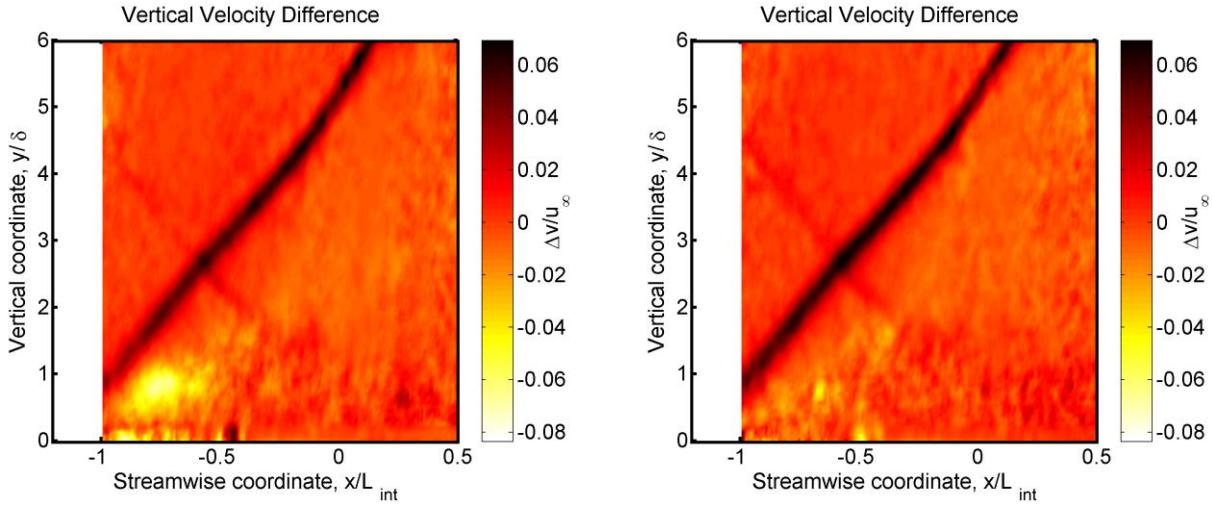

a) Phase 1 **b) Phase 2**

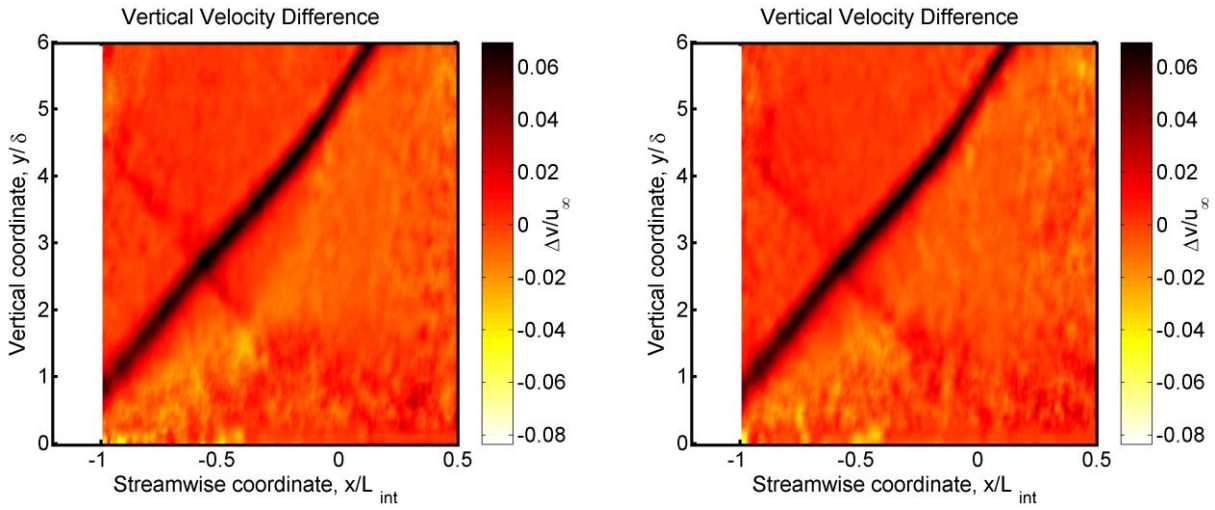

c) Phase 3 **d) Phase 4**

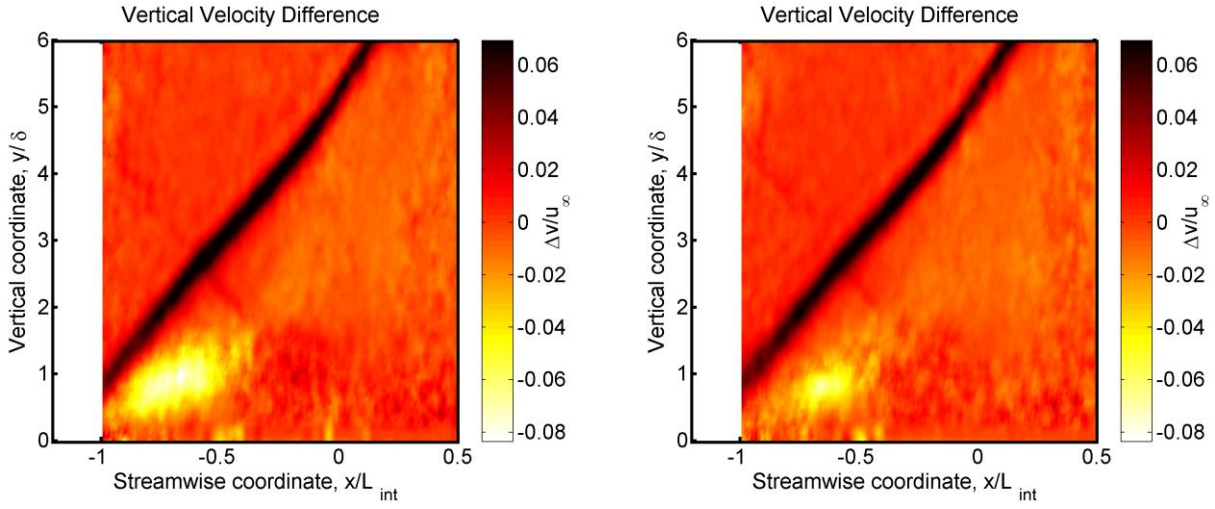

e) Phase 5 **f) Phase 6**

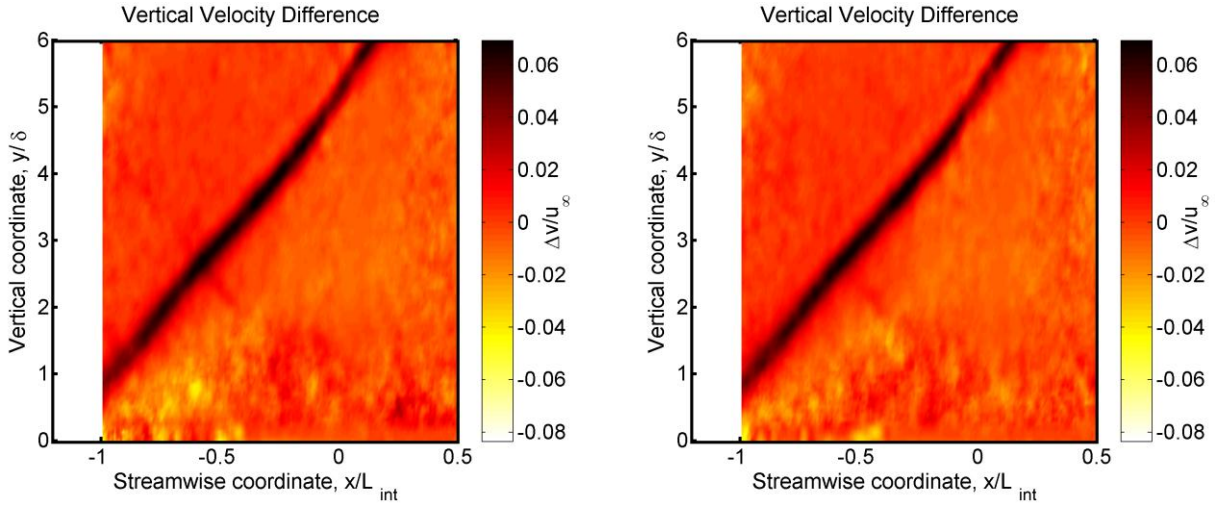

g) Phase 7 **h) Phase 8**

Figure 10: St_F = 0.03, DC = 50% Phase Sweep

It was not clear from the above results whether the LAFPAs were forcing an instability, or whether the observed effects were merely due to local heating of the flow (energy addition). For the excitation of an instability, the location of actuation is critical, and the effect is maximized when actuation is at the maximum receptivity location. Thus, it was decided to vary the LAFPAs' location to investigate whether perhaps the LAFPAs were simply not close to the receptivity location, which is expected to be just upstream of the separation location in this case. Still operating under the assumption that the sensitive region would be in the vicinity of the separation line (shear layer origin) the LAFPAs' streamwise location was varied from $X_a^* = -1.09$ to $X_a^* = -0.77$ (see Figure 11). Surprisingly almost no difference in the LAFPAs' effectiveness was observed among the locations tested. Thus, the rest of the experiments were performed with the LAFPAs located at $X_a^* = -0.96$ (see Figure 11).

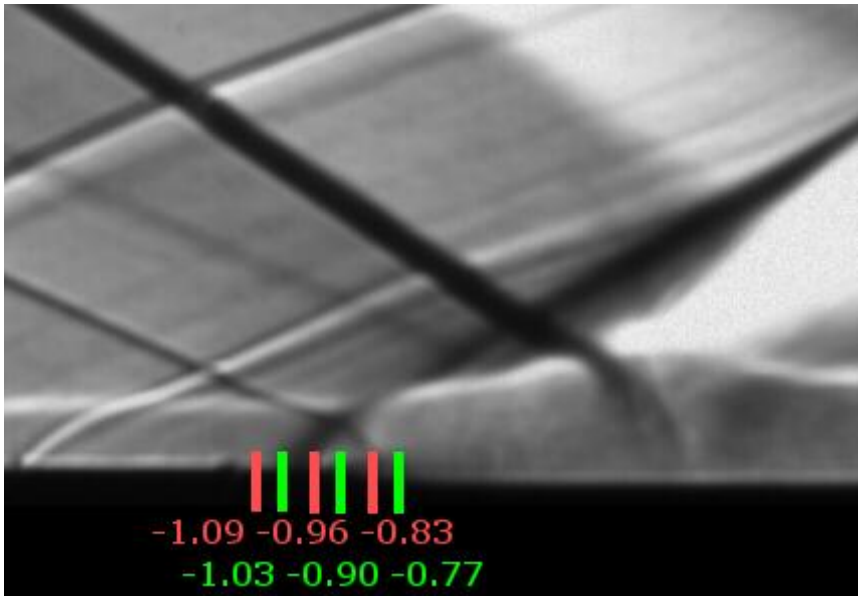

Figure 11: Schlieren Image Showing the Various Tested Streamwise Locations of the LAFPAs

The frequency dependence of the control authority was also investigated. The frequency of the actuators was varied from $St_F = 0.0075$ to $St_F = 1.5$. Figure 12 shows velocity difference maps for two phases: the phase of "maximum displacement" and "maximum relaxation" (corresponding to minimum displacement). Due to the response time of the flow, which phase corresponds to maximum displacement or relaxation varies as a function of frequency. A comparison of the maximum displacement data shows a slight increase in upstream displacement as the actuator frequency is increased. In contrast, the maximum relaxations show a marked increase in shock displacement with increasing frequency. This appears to be consistent with the results of the initial LAFPA forcing (Figure 10). Higher frequencies have shorter periods, which means there is less time for the reflected shock to relax while the LAFPAs are not firing. This explains the behavior of the maximum relaxation. The maximum displacement trend follows a similar idea: the reflected shock is moved upstream by the actuators, and due to the smaller relaxation time at high frequencies, the maximum relaxation point is further upstream, thus resulting in a greater maximum displacement. Although this reasoning makes sense, the trend is slightly confusing given the significantly longer firing-time present at the lower frequencies. This may be indicative of some sort of saturation occurring when forcing at low frequencies.

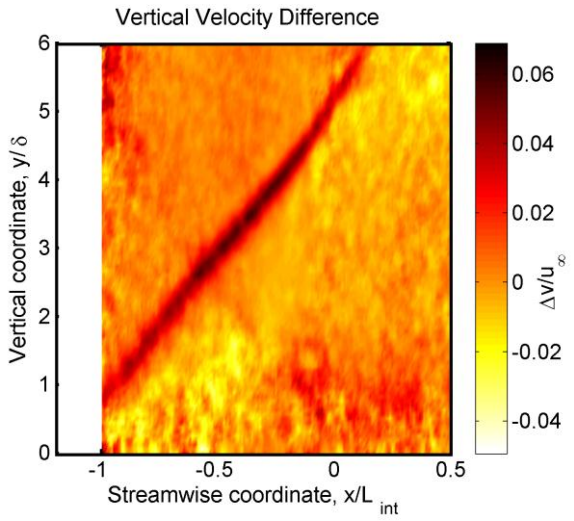

a) St = 0.0075, Max. Displacement

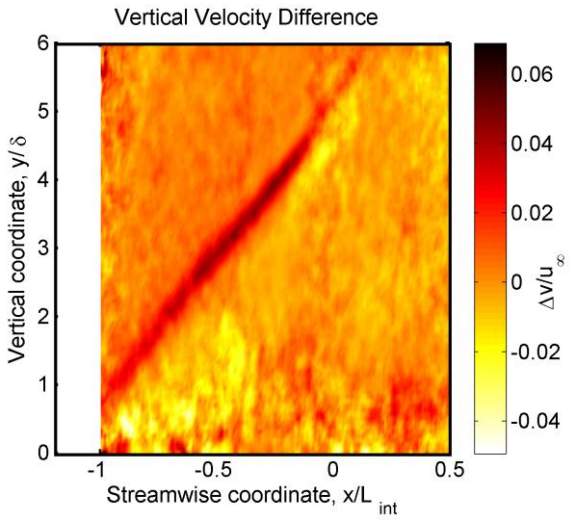

b) St = 0.0075, Max. Relaxation

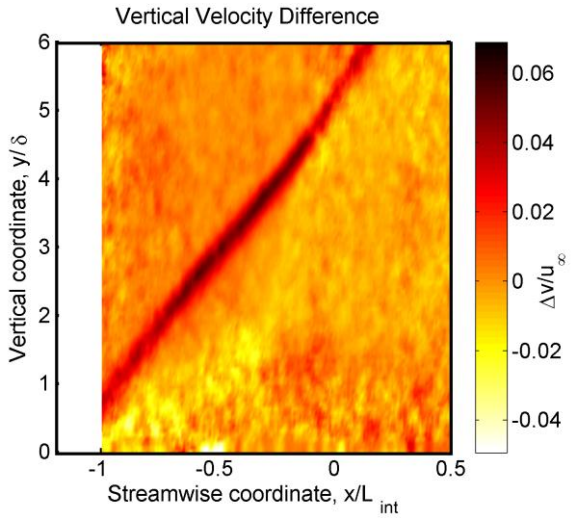

c) St = 0.03, Max. Displacement

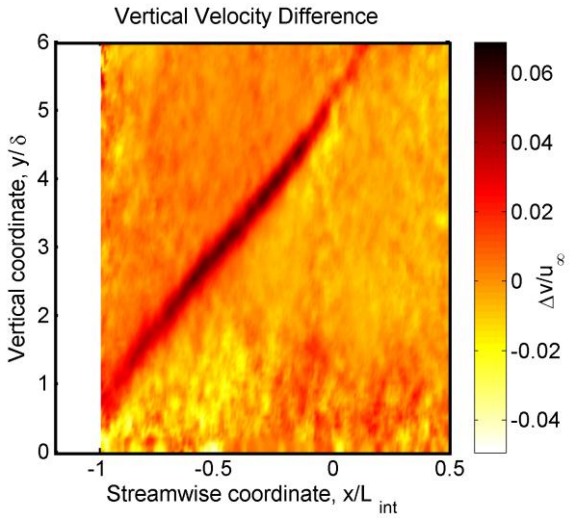

d) St = 0.03, Max. Relaxation

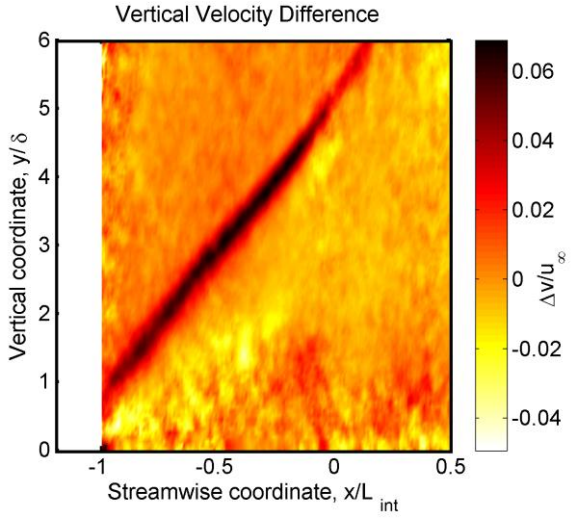

e) St = 0.48, Max. Displacement

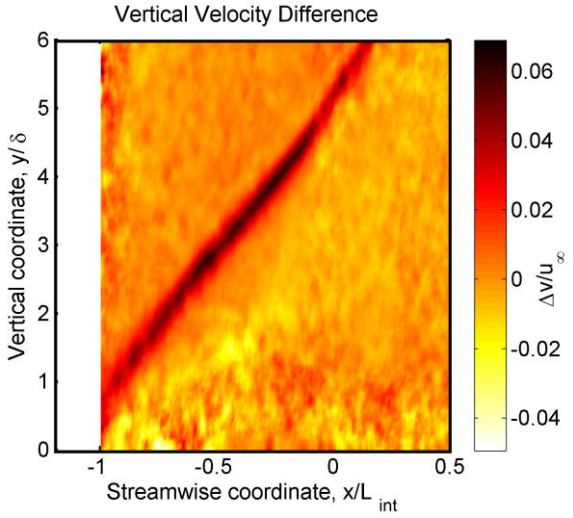

f) St = 0.48, Max. Relaxation

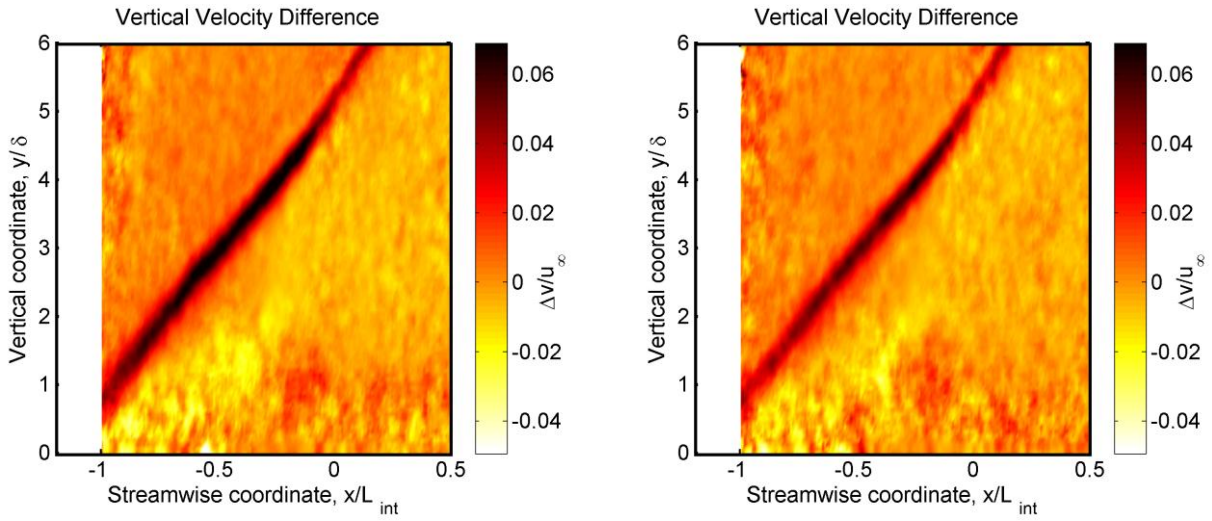

g) St = 1.5, Max. Displacement **h) St = 1.5, Max. Relaxation**

Figure 12: The Effects Forcing Strouhal Number on the Maximum Displacement and Relaxation

It was also of interest to learn how the duty cycle of the LAFPAs affected their control authority. The actuators were operated at duty cycles of 10%, 30%, and 50%. The velocity maps corresponding to the maximum displacement and relaxation are shown in Figure 13. This study was performed for an actuator frequency of St_F = 0.03. An inspection of the results shows clearly that a higher duty cycle results in greater displacement at both phases. This seems intuitive given what was found in the frequency sweep. Namely, a longer duty cycle results in more time spent firing, therefore the overall shock displacement is greater because it does not relax as far. Moreover each time the LAFPAs begin firing the reflected shock position is further upstream due to the smaller relaxation time. Furthermore, a longer firing time may allow the displacement to saturate rather than stopping actuation when the reflected shock has only moved upstream partway.

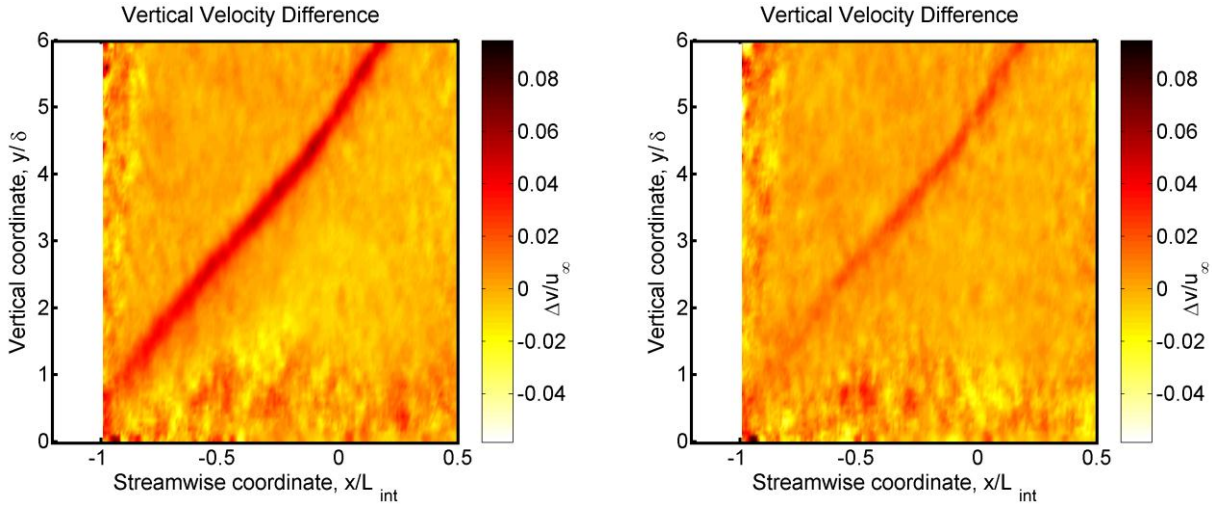

a) DC = 10%, Max. Displacement **b) DC = 10%, Max. Relaxation**

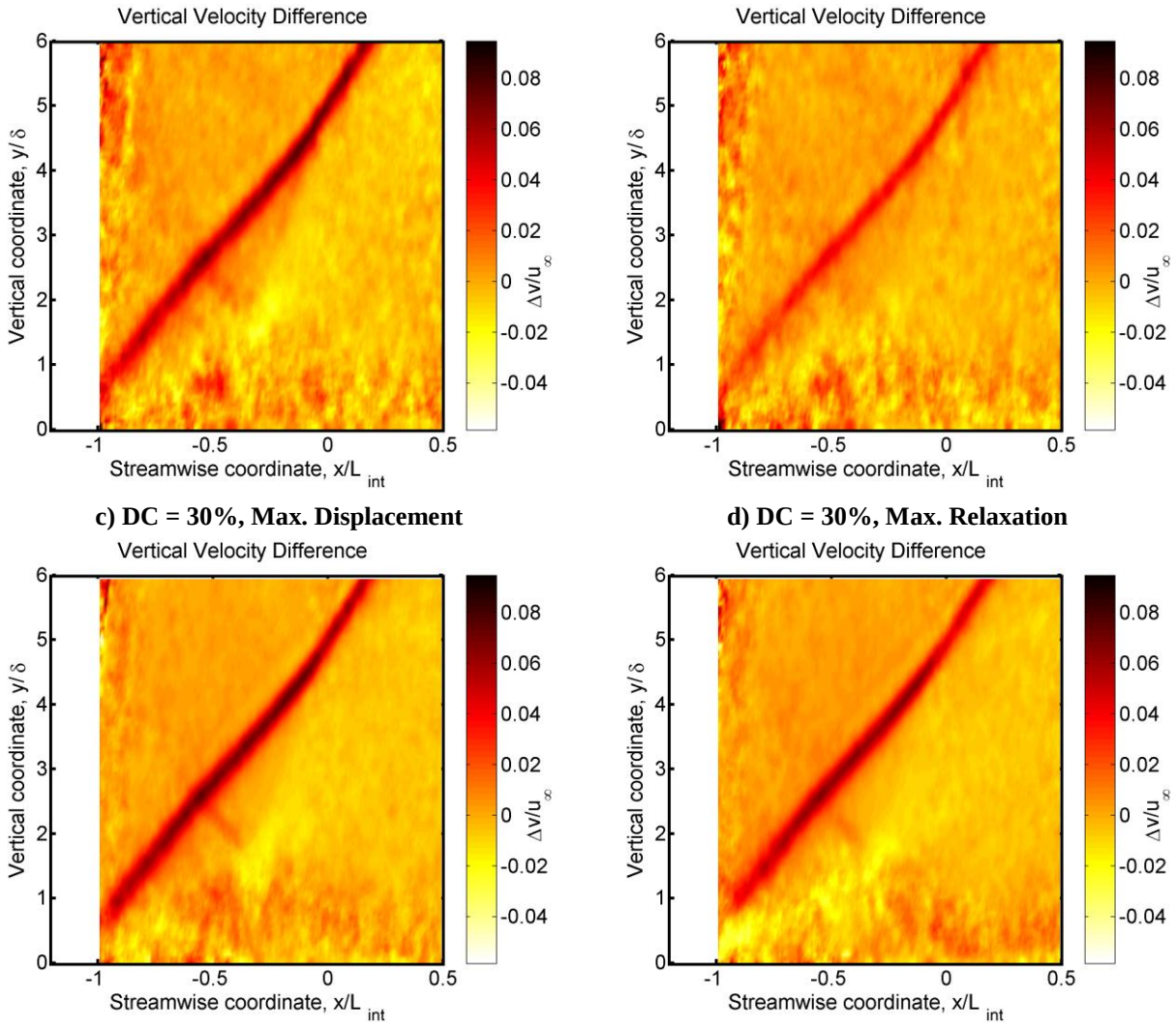

c) DC = 30%, Max. Displacement **d) DC = 30%, Max. Relaxation**

e) DC = 50%, Max. Displacement **f) DC = 50%, Max. Relaxation**

Figure 13: The Effects Forcing Duty Cycle on the Maximum Displacement and Relaxation

The effect of the LAFPAs on the downstream profiles was also investigated. As previously mentioned (see Baseline Characterization) the impingement of the expansion fan near the downstream end of the interaction makes the determination of the actual performance of the LAFPAs in a supersonic inlet difficult. However, a comparison of the baseline to the forced cases can still yield semi-quantitative information regarding the LAFPAs' overall effects on the recovering boundary layer. When comparing downstream velocity profiles from the forced data to the baseline (not shown), it appeared that the LAFPAs were actually improving the downstream flow. The downstream profiles of the forced cases were fuller and less distorted than those of the baseline.

Due to the reflected shock being moved upstream, great care was taken when comparing downstream profiles. It seemed likely that, because the interaction was being shifted upstream the benefits of the LAFPAs might be due solely to the fact that the forced boundary layer has had more time to recover than the baseline. In order to check if this was the case each profile in the forced case was matched to the most similar profile in the baseline case. The best match for the forced profiles was found to be consistently 5 mm upstream. This is approximately the same distance by which the shock was displaced upstream. Thus, it was concluded that the apparent beneficial effect of the LAFPAs on the downstream profile was simply due to a lateral shift in the recovering boundary layer.

F. Mechanism Discussion

When examining a new active control technique it is generally helpful to understand the physics behind how it exerts control. This allows the search for the optimum forcing parameters to be more efficiently conducted. It is thus

of interest to give thought to how the LAFPAs are introducing changes to the SWBLI. The starting hypothesis of this work was that the actuators would manipulate the low frequency instabilities that were naturally present in the upstream portion of the interaction region to generate large changes with minimal power input. However, the results (see LAFPA Control Authority) do not appear to support this hypothesis.

When manipulating a natural instability, as with any system, there is a frequency (or a set or range of frequencies) at which perturbations naturally produce a greater effect. As a result of this, there is often a forcing frequency at which effectiveness is maximized. This study sought to manipulate the low frequency unsteadiness associated with the upstream region of the interaction. Using that hypothesis as the focus of the research did not identify a "peak-effectiveness" frequency, rather it appears that increasing the frequency increases the effectiveness. It could perhaps be argued that no peak was discovered because the highest tested frequency was not sufficiently high. If this is the case, however, it is not immediately apparent what the natural manifestation of the forced instability is. It is known that there are natural oscillations between St = 0.03 and 0.5; however, apart from the upstream boundary layer turbulence (St ~ 7) there are no other notable oscillations of frequency higher than the highest tested forcing frequency: St_F = 1.5. Thus, it seems likely that no peak effectiveness frequency was discovered because one does not exist (for this physical configuration). Locating and forcing with the LAFPAs in an attempt to influence the downstream, intermediate frequency instability could provide a more beneficial control result.

Varying the LAFPAs' streamwise location also yielded interesting results. Namely, within the tested region there was little or no variation in the LAFPAs' effectiveness. The nature of natural instabilities is spatially sensitive in the sense that the developing flow patterns will affect the same perturbations differently depending on where they are introduced. The result of this is that a particular instability will have a "sensitive" region, termed the receptivity region, where introduced perturbations can have a large effect. If introduced far from this region the perturbations will not cause significant changes in the flow. Thus, it seems logical that changing the actuator location should result in a change in effectiveness. The LAFPAs streamwise location was varied over a range of potential receptivity associated with the low frequency oscillation. However, it seems unlikely that there would not even be a slight change or trend in observed effectiveness.

These two results seem to indicate clearly that the shock displacement is not being affected through the postulated instability manipulation. If this is the case, then what is the LAFPAs' control mechanism? Work by Jaunet et al.[40] has shown that heating the upstream boundary layer moves the reflected shock upstream. They suggest that this is a result of the change in density introduced by the heating. The density changes affect the mass balance within the separation bubble resulting in a spatially expanded bubble. This effect is similar to what has been observed in this work. The idea of heating being the control mechanism seems to fit well with the lack of dependence on location (as long as the LAFPAs are upstream of the separation) and the observed dependence on frequency, i.e. given less time not firing (when no heat is added to the flow) the displacement is greater. This also makes sense given the observed increasing displacement with increasing duty cycle (time averaged power addition). However, the heating/energy imparted to the flow by LAFPAs is estimated to be nearly two orders of magnitude less than that used by Jaunet et al.[40] This difference could be due to the energy density of the actuators compared to a heated wall. More work is required to conclusively determine the LAFPAs' control mechanism.

Conclusions

LAFPAs were investigated as a potential SWBLI control method for mixed-compression inlet flow control. This was achieved by examining the effects of the actuators on a single oblique, impinging SWBLI. Before examining the LAFPAs' control authority the tunnel flow was characterized and found to agree well with what has previously been observed in literature. In addition a comparison of the unsteadiness from the ramp generated SWBLI was found to be similar to the previously wedge generated interaction.

Forcing with the LAFPAs was observed to move the reflected shock upstream by about a boundary layer thickness (~5 mm). Phase locked data showed that the displacement was greatest during the part of the forcing period that the LAFPAs were firing. In addition, the LAFPAs' control authority was found not to depend on streamwise location within the range tested and to increase with increasing frequency and duty cycle. These trends are difficult to explain if the LAFPAs' control mechanism is natural instability manipulation. If, however, the LAFPAs are merely heating the flow this behavior makes much more sense, even though the imparted energy to the flow by LAFPAs is two orders of magnitude less than what has been used in the literature. Thus, it is tentatively suggested that the LAFPAs are perhaps not manipulating instabilities, but rather altering the density profile of the upstream boundary layer resulting in a shifted separation.

Acknowledgments

The generous support of this work by the Air Force Office of Scientific Research (Dr. John Schmisseur) and the Air Force Research Laboratory (Mr. Jon Tinapple) is gratefully acknowledged.

References

[1] Surber, L. E., and J. A. Tinapple. "Inlet Flow Control Technology: Learning from History, Reinventing the Future." *50th AIAA Aerospace Sciences Meeting*. AIAA 2012-0012.

[2] Syberg, J., and J. L. Koncsek. "Experimental Evaluation of an Analytically Derived Bleed System for a Supersonic Inlet." *Journal of Aircraft* 13.10 (1976): 792-97.

[3] Baruzzini, D. "An Industry Perspective on the Role of Bleed in High-Speed Inlet Design Process." 5th Annual Shock Wave/Boundary Layer Interaction Workshop. 2012.

[4] Touber, E., and N. D. Sandham. "Large-Eddy Simulation of Low-Frequency Unsteadiness in a Turbulent Shock-Induced Separation Bubble." *Theoretical and Computational Fluid Dynamics* 23 (2009): 79-107.

[5] Shahneh, A., and F. Motallebi. "Effect of Submerged Vortex Generators on Shock-Induced Separation in Transonic Flow." *Journal of Aircraft* 46.3 (2009): 856-63.

[6] Anderson, B. H., J. Tinapple, and L. Surber. "Optimal Control of Shock Wave Turbulent Boundary Layer Interactions Using Micro-Array Actuation." *3rd Flow Control Conference*. 2006-3197.

[7] Babinsky, H., Y. Li, and C. P. Ford. "Microramp Control of Supersonic Oblique Shock-Wave/Boundary-Layer Interactions." *AIAA Journal* 47.3 (2009): 668-75.

[8] Lee, S., M. Goettke, E. Loth, J. Tinapple, and J. Benek. "Microramps Upstream of an Oblique-Shock/Boundary-Layer Interaction." *AIAA Journal* 48.1 (2010): 104-18.

[9] Lee, S., E. Loth, and H. Babinsky. "Normal Shock Boundary Layer Control with Various Vortex Generator Geometries." *AIAA 5th Flow Control Conference*. 2010-4254.

[10] Babinsky, H., and H. Ogawa. "SBLI Control for Wings and Inlets." *Shock Waves* 18.2 (2008): 89-96.

[11] Gefroh, D., E. Loth, C. Dutton, and S. McIlwain. "Control of an Oblique Shock/Boundary-Layer Interaction with Aeroelastic Mesoflaps." *AIAA Journal* 40.12 (2002): 2456-66.

[12] Kalra, C. S., S. H. Zaidi, R. B. Miles, and S. O. Macheret. "Shockwave-Turbulent Boundary Layer Interaction Control Using Magnetically Driven Surface Discharges." *Experiments in Fluids* 50 (2011): 547-59.

[13] Souverein, L. J., and J.-F. Debiève. "Effect of Air Jet Vortex Generators on a Shock Wave Boundary Layer Interaction." *Experiments in Fluids* 49 (2010): 1053-64.

[14] Narayanaswamy, V., N. Clemens, and L. Raja. "Investigation of a Pulsed-Plasma Jet for Shock/Boundary Layer Control." *AIAA 48th Aerospace Sciences Meeting*. 2010-1089.

[15] Dolling, D., and L. Brusniak. "Separation Shock Motion in Fin, Cylinder, and Compression Ramp-Induced Turbulent Interactions." *AIAA Journal* 27.6 (1989): 734-42.

[16] Dupont, P., C. Haddad, and J. F. Debiève. "Space and Time Organization in a Shock-Induced Separated Boundary Layer." *Journal of Fluid Mechanics* 559 (2006): 255-77.

[17] Dolling, D. "Fifty Years of Shock-Wave/Boundary-Layer Interaction Research: What Next?" *AIAA Journal* 39.8 (2001): 1517-31.

[18] Andreopoulos, J., and K. C. Muck. "Some New Aspects of the Shock-Wave/Boundary-Layer Interaction in Compression-Ramp Flows." *Journal of Fluid Mechanics* 180 (1987): 405-28.

[19] Ganapathisubramani, B., N. Clemens, and D. Dolling. "Low-Frequency Dynamics of Shock-Induced Separation in a Compression Ramp Interaction." *Journal of Fluid Mechanics* 636 (2009): 397-425.

[20] Beresh, S. J., J. F. Henfling, R. W. Spillers, and B. O. M. Pruett. "Very-Large-Scale Coherent Structures in the Wall Pressure Field beneath a Supersonic Turbulent Boundary Layer." *49th AIAA Aerospace Sciences Meeting*. 2011-746.

[21] Piponniau, S., J. Dussauge, J. Debieve, and P. Dupont. "A Simple Model for Low-Frequency Unsteadiness in Shock-Induced Separation." *Journal of Fluid Mechanics* 629 (2009): 87-108.

[22] Pirozzoli, S., and F. Grasso. "Direct Numerical Simulation of Impinging Shock Wave/Turbulent Boundary Layer Interaction at M=2.25." *Physics of Fluids A* 18 (2006): 1-17.

[23] Narayanaswamy, V. "Investigation of a Pulsed-Plasma Jet for Separation Shock/Boundary Layer Interaction Control." University of Texas at Austin, 2010. Print.

[24] Touber, E., and N. D. Sandham. "Low-Order Stochastic Modelling of Low-Frequency Motions in Reflected Shock-Wave/Boundary-Layer Interactions." *Journal of Fluid Mechanics* 671 (2011): 417-65.

[25] Little, J., K. Takashima, M. Nishihara, I. Adamovich, and M. Samimy. "Separation Control with Nanosecond-Pulse-Driven Dielectric Barrier Discharge Plasma Actuators." *AIAA Journal* 50.2 (2012): 350-65.

[26] Rethmel, C., J. Little, K. Takashima, A. Sinha, I. Adamovich, and M. Samimy. "Flow Separation Control over an Airfoil with Nanosecond Pulse Driven DBD Plasma Actuators." *49th AIAA Aerospace Sciences Meeting*. 2011-0487.
[27] Barter, J. W., and D. S. Dolling. "Reduction of Fluctuating Pressure Loads in Shock/Boundary-Layer Interactions Using Vortex Generators." *AIAA Journal* 33.10 (1995): 1842-49.
[28] Utkin, Y. G., S. Keshav, J.-H. Kim, J. Kastner, I. V. Adamovich, and M. Samimy. "Development and Use of Localized Arc Filament Plasma Actuators for High-Speed Flow Control." *Journal of Physics D: Applied Physics* 40.3 (2007): 685-94.
[29] Samimy, M., J.-H. Kim, J. Kastner, I. Adamovich, and Y. Utkin. "Active Control of a Mach 0.9 Jet for Noise Mitigation Using Plasma Actuators." *AIAA Journal* 45.4 (2007): 890-901.
[30] Samimy, M., J.-H. Kim, J. Kastner, I. Adamovich, and Y. Utkin. "Active Control of High-Speed and High-Reynolds-Number Jets Using Plasma Actuators." *Journal of Fluid Mechanics* 578.1 (2007): 305-30.
[31] Sinha, A., K. Kim, J.-H. Kim, A. Serrani, and M. Samimy. "Extremizing Feedback Control of a High-Speed and High Reynolds Number Jet." *47th AIAA Aerospace Sciences Meeting*. 2009-0849.
[32] Titchener, N., H. Babinsky, and E. Loth. "Can Fundamental Shock-Wave/Boundary-Layer Interaction Research Be Relevant to Inlet Aerodynamics?" *50th AIAA Aerospace Sciences Meeting*. AIAA 2012-0017.
[33] Caraballo, E., N. Webb, J. Little, J.-H. Kim, and M. Samimy. "Supersonic Inlet Flow Control Using Plasma Actuators." *47th AIAA Aerospace Sciences Meeting*. 2009-924.
[34] Webb, N., C. Clifford, and M. Samimy. "Preliminary Results on Shock Wave/Boundary Layer Interaction Control Using Localized Arc Filament Plasma Actuators." *41st AIAA Fluid Dynamics Conference*. 2011-3426.
[35] Burton, D., H. Babinsky, and P. Bruce. "Experimental Investigations into Parameters Governing Corner Interaction for Transonic Shock Wave/Boundary Layer Interactions." *48th AIAA Aerospace Sciences Meeting*. 2010-0871.
[36] Burton, D., and H. Babinsky. "Normal Shock Interactions in Rectangular Channels." *50th AIAA Aerospace Sciences Meeting*. AIAA 2012-1114.
[37] Baruzzini, D., N. Domel, and D. N. Miller. "Addressing Corner Interactions Generated by Oblique Shock-Waves in Unswept Right-Angle Corners and Implications for High-Speed Inlets." *50th AIAA Aerospace Sciences Meeting*. AIAA 2012-0275.
[38] Maise, G., and H. McDonald. "Mixing Length and Kinematic Eddy Viscosity in a Compressible Boundary Layer." *AIAA Journal* 6.1 (1968): 73-80.
[39] Babinsky, H., and J. K. Harvey. *Shock Wave-Boundary-Layer Interactions*. New York, New York: Cambridge University Press, 2011. Print.
[40] Jaunet, V., J. F. Debiève, and P. Dupont. "Experimental Investigation of an Oblique Shock Reflection with Separation over a Heated Wall." *50th AIAA Aerospace Sciences Meeting*. AIAA 2012-1095.